


Article

Dritsite, $\text{Li}_2\text{Al}_4(\text{OH})_{12}\text{Cl}_2 \cdot 3\text{H}_2\text{O}$, a New Gibbsite-Based Hydrotalcite Supergroup Mineral

Elena S. Zhitova ^{1,2,*} , Igor V. Pekov ³, Ilya I. Chaikovskiy ⁴, Elena P. Chirkova ⁴,
Vasily O. Yapaskurt ³, Yana V. Bychkova ³, Dmitry I. Belakovskiy ⁵, Nikita V. Chukanov ⁶,
Natalia V. Zubkova ³, Sergey V. Krivovichev ^{1,7} and Vladimir N. Bocharov ⁸

¹ Department of Crystallography, St. Petersburg State University, Universitetskaya nab. 7/9, St. Petersburg 199034, Russia

² Laboratory of Mineralogy, Institute of Volcanology and Seismology, Russian Academy of Sciences, Bulvar Piypa 9, Petropavlovsk-Kamchatsky 683006, Russia

³ Faculty of Geology, Moscow State University, Vorobievy Gory, Moscow 119991, Russia

⁴ Mining Institute, Ural Branch of the Russian Academy of Sciences, Sibirskaia str., 78a, Perm 614007, Russia

⁵ Fersman Mineralogical Museum, Russian Academy of Sciences, Leninsky Prospekt 18-2, Moscow 119071, Russia

⁶ Institute of Problems of Chemical Physics, Russian Academy of Sciences, Akad. Semenova 1, Chernogolovka, Moscow Region 142432, Russia

⁷ Nanomaterials Research Centre, Kola Science Centre, Russian Academy of Sciences, Fersman Street 14, Apatity 184209, Russia

⁸ Resource Center Geomodel, St. Petersburg State University, Universitetskaya nab. 7/9, St. Petersburg 199034, Russia

* Correspondence: zhitova_es@mail.ru; Tel.: +7-924-587-51-91

Received: 2 August 2019; Accepted: 14 August 2019; Published: 17 August 2019



Abstract: Dritsite, ideally $\text{Li}_2\text{Al}_4(\text{OH})_{12}\text{Cl}_2 \cdot 3\text{H}_2\text{O}$, is a new hydrotalcite supergroup mineral formed as a result of diagenesis in the halite–carnallite rock of the Verkhnekamskoe salt deposit, Perm Krai, Russia. Dritsite forms single lamellar or tabular hexagonal crystals up to 0.25 mm across. The mineral is transparent and colourless, with perfect cleavage on {001}. The chemical composition of dritsite (wt. %; by combination of electron microprobe and ICP–MS; H_2O calculated by structure refinement) is: Li_2O 6.6, Al_2O_3 45.42, SiO_2 0.11, Cl 14.33, SO_3 0.21, $\text{H}_2\text{O}_{\text{calc}}$ 34.86, $\text{O} = \text{Cl} - 3.24$, total 98.29. The empirical formula based on $\text{Li} + \text{Al} + \text{Si} = 6$ apfu (atom per formula unit) is $\text{Li}_{1.99}\text{Al}_{4.00}\text{Si}_{0.01}[(\text{OH})_{12.19}\text{Cl}_{1.82}(\text{SO}_4)_{0.01}]_{\Sigma 14.02} \cdot 2.60(\text{H}_2\text{O})$. The Raman spectroscopic data indicate the presence of O–H bonding in the mineral, whereas CO_3^{2-} groups are absent. The crystal structure has been refined in the space group $P6_3/mcm$, $a = 5.0960(3)$, $c = 15.3578(13)$ Å, and $V = 345.4(5)$ Å³, to $R_1 = 0.088$ using single-crystal data. The strongest lines of the powder X-ray diffraction pattern (d , Å (I , %) (hkl)) are: 7.68 (100) (002), 4.422 (61) (010), 3.832 (99) (004, 012), 2.561 (30) (006), 2.283 (25) (113), and 1.445 (26) (032). Dritsite was found as 2H polytype, which is isotypic with synthetic material and shows strong similarity to chlormagalumite-2H. The mineral is named in honour of the Russian crystallographer and mineralogist Prof. Victor Anatol'evich Drits.

Keywords: dritsite; hydrotalcite supergroup; lithium aluminium hydroxide; layered double hydroxide; gibbsite-derived; crystal structure; evaporitic salt rock; Verkhnekamskoe potassium salt deposit; Perm Krai

1. Introduction

In this paper we provide a description of the new hydrotalcite supergroup mineral dritsite. Hydrotalcite supergroup minerals are commonly known as layered double hydroxides (LDHs), i.e.,

hydroxides containing two cations, usually di- and trivalent [1–3], although a group of synthetic LiAl_2 -based LDHs is also known [4–19]. Currently, forty-four hydrotalcite supergroup minerals are known, including some that are questionable as mineral species [3]. All of them, excluding mössbauerite, are composed of di- and trivalent cations, whereas mössbauerite contains only Fe^{3+} [20]. The new monoclinic mineral akopovaite, recently approved by the IMA–CNMNC (International Mineralogical Association, Commission on new minerals, nomenclature and classification) (IMA2018-095, [21]), has the chemical formula $\text{Li}_2\text{Al}_4(\text{OH})_{12}\text{CO}_3 \cdot 3\text{H}_2\text{O}$, however, its full description has not yet been published. Thus, here we provide the first description of this natural LiAl_2 -based LDH. The crystal structures of all currently known hydrotalcite supergroup members are based on brucite-type layers (Figure 1), where some of M^{2+} cations are replaced by M^{3+} . A strong predominance of M^{2+} cations over M^{3+} is observed, with the most common $M^{2+}:M^{3+}$ ratios being 2:1 and 3:1. The crystal structures of LiAl_2 -LDHs are based upon gibbsite-derived dioctahedral layers of $\text{Al}(\text{OH})_6$ octahedra, with vacant octahedral sites occupied by Li^+ cations (Figure 1). The $[\text{LiAl}_2(\text{OH})_6]^+$ octahedral layers alternate, with negatively charged interlayer constituents represented by anions Cl^- , CO_3^{2-} , SO_4^{2-} , and H_2O groups.

The new mineral is named in honour of the Russian crystallographer and mineralogist Victor Anatol'evich Drits (ВикторАнато́льевич Дри́тс) (born 1932) from Geological Institute of the Russian Academy of Sciences, Moscow, Russia. Prof. Drits is an outstanding specialist in mineralogy of sedimentary rocks and crystal chemistry of compounds with layered structures, especially clay minerals. He contributed greatly to the development of new scientific methods and approaches for the studies of crystal chemistry and systematics of layered minerals, including hydrotalcite supergroup members [22,23]. The mineral and its name have been approved by the IMA–CNMNC (IMA2019-017).

The type material is deposited in the collections of the Fersman Mineralogical Museum of the Russian Academy of Sciences, Moscow, Russia, under the registration number 5380/1.

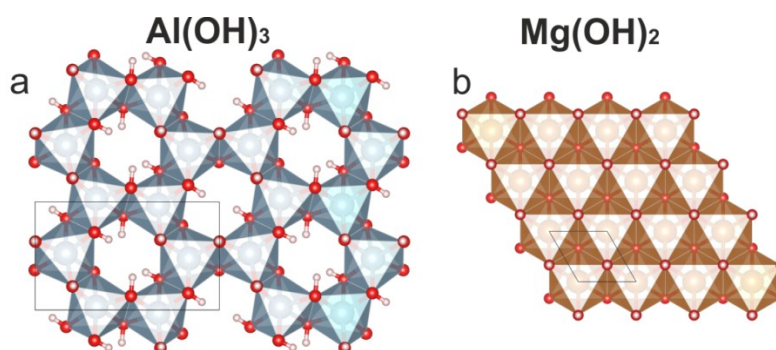


Figure 1. (a) The dioctahedral layer in the crystal structure of gibbsite [24] composed of $\text{Al}(\text{OH})_6$ octahedra and containing vacancies. (b) The trioctahedral layer in the crystal structure of brucite [25] composed of $\text{Mg}(\text{OH})_6$ octahedra as a main structural unit of LDHs composed of di- and trivalent cations (all currently known hydrotalcite supergroup members).

2. Materials and Methods

2.1. Occurrence, Appearance, Physical Properties, and Optical Data

Dritsite was found in the core of the borehole #2001, at a depth of 247.6–248 m, drilled at the Romanovskiy area of the well-known giant Verkhnekamskoe potassium salt deposit, 30-km south of the city of Berezniki, Perm Krai, Western Urals, Russia [26–28]. The new mineral was found in a halite–carnallite rock in association with dolomite, magnesite, quartz, Sr-bearing baryte, kaolinite, potassic feldspar, krasnoshteinite, $\text{Al}_8[\text{B}_2\text{O}_4(\text{OH})_2](\text{OH})_{16}\text{Cl}_4 \cdot 7\text{H}_2\text{O}$ (IMA2018-077) [29], congolite, members of the goyazite–woodhouseite series, fluorite, hematite, and anatase. We believe that dritsite was formed as a result of diagenetic or post-diagenetic processes in a halite–carnallite evaporitic rock belonging to Layer E of the Verkhnekamskoe deposit.

Dritsite forms separate lamellar to tabular hexagonal crystals flattened on {001} up to 0.25 mm across and up to 0.02 mm thick and their parallel intergrowths (Figure 2). The pinacoid {0001} is the major crystal form. The hexagonal prism {1100} is the most typical lateral form, whereas the hexagonal prism {10-10} faces are rare and minor; faces of hexagonal dipyramids $\{hh(-2h)l\}$, and occasionally $\{h0il\}$, were observed but not indexed. Crystals shown in Figure 2 were separated after dissolution of the host halite–carnallite rock in cold water. The mineral is colorless with a white streak and vitreous luster. The Mohs hardness is approximately 2 (by comparison with other hydrotalcite supergroup minerals). The mineral has a perfect mica-like cleavage on {001} and a laminated fracture. The crystals are easily bent but are non-resilient. The mineral is non-fluorescent in the ultraviolet light. The density could not be measured because of the paucity of material; the density calculated using the empirical formula and the unit-cell parameters determined from single-crystal X-ray diffraction data is 2.123 g/cm³. Dritsite is insoluble in water.

The mineral is optically uniaxial (+), $\epsilon = 1.583(2)$, and $\omega = 1.546(2)$ (589 nm). Under a microscope it is colorless and non-pleochroic. The Gladstone–Dale compatibility index [30] is $1 - (K_P/K_C) = -0.001$ (superior).

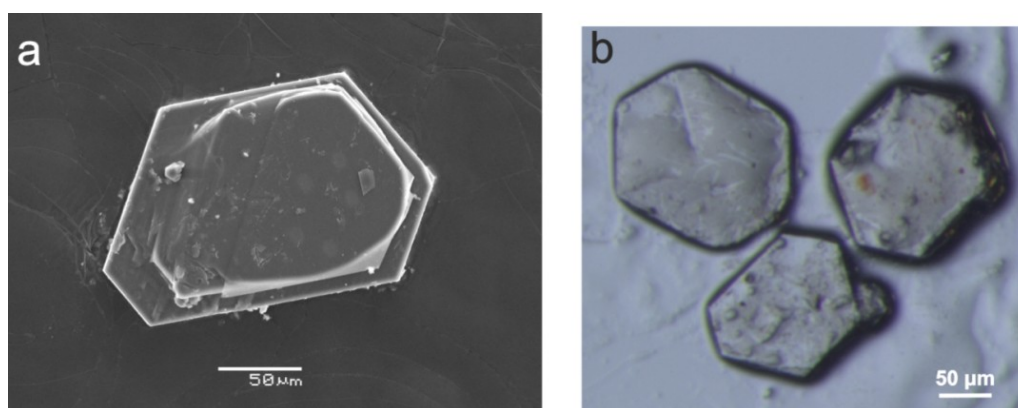


Figure 2. Crystals of dritsite: (a) secondary electron image; (b) photomicrograph in unpolarized visible light.

2.2. Chemical Composition

The chemical composition of dritsite was studied using a Jeol JSM-6480LV scanning electron microscope equipped with an INCA-Wave 500 wavelength-dispersive spectrometer (Laboratory of Analytical Techniques of High Spatial Resolution, Department of Petrology, Moscow State University, Moscow, Russia). Electron microprobe analyses (5) were obtained in the wavelength-dispersive spectroscopy mode (20 kV and 20 nA; the electron beam was rastered to a $5 \times 5 \mu\text{m}$ area) and given contents of Al, Si, S, and Cl. The standards used were: Al_2O_3 (Al), wollastonite (Si), SrSO_4 (S), and NaCl (Cl). The content of other elements with atomic numbers higher than 8 is below the detection limit.

The Li content was determined using inductively coupled plasma mass spectrometry (ICP–MS). The measurements were carried out with an Element-2 (Thermo Fisher Scientific, Moscow, Russia) instrument, which had a high resolution (that avoids interference of components) and sensitivity. Several crystals of the mineral were dissolved in 10 cm³ of 3% HNO_3 solution (Merck, Suprapur®, Darmstadt, Germany) in deionized water (EasyPure, Moscow, Russia). Since the mass of the sample was too low for accurate weighing, we have determined contents of Li and Al in relative units and further used the average Al content, obtained by electron microprobe, for calculation of the Li content. The obtained value is in good agreement with the Li content determined from the crystal-structure refinement.

The H_2O content was not determined because of the paucity of the material but was calculated based on the crystal-structure data (see below) and by considering the charge-balance requirements (for OH groups). The analytical total (98.29 wt. %) was close to 100 wt. %, which demonstrated the

agreement between the electron microprobe data for Al, Si, S, and Cl, the ICP–MS data for Li, and the H₂O content calculated from the crystal-structure data.

2.3. Raman Spectroscopy

The Raman spectra of dritsite were obtained with a spectrometer Horiba Jobin-Yvon LabRam HR 800 (Geomodel Resource Center, St. Petersburg State University, St. Petersburg, Russia) equipped with an Ar⁺ laser ($\lambda = 514$ nm) at 50 mW output power. The spectra were recorded at room temperature from the cleavage plane and an edge of the plate and were further processed using LabSpec and Origin software.

2.4. Single-Crystal X-ray Diffraction and Crystal Structure Determination

Single-crystal X-ray diffraction data were collected by means of an Xcalibur S charge-coupled device (CCD) diffractometer (Faculty of Geology, Moscow State University, Moscow, Russia) operated at 40 kV and 50 mA using MoK α radiation. The data were integrated and corrected for absorption using a multi-scan model and the CrysAlisPro program [31]. The crystal structure was solved and refined with the ShelX (Version 2016, ShelX, Göttingen, Germany) program package using direct methods [32].

2.5. Powder X-ray Diffraction

Powder X-ray diffraction data (PXRD) were collected by means of a Rigaku R-Axis Rapid II (X-ray Diffraction Resource Center, St. Petersburg State University, St. Petersburg, Russia) diffractometer (Debye-Scherrer geometry, $d = 127.4$ mm) equipped with a rotating anode X-ray source (CoK α , $\lambda = 1.79021$ Å) and a curved image plate detector. The data were integrated using the software package Osc2Tab/SQRay [33]. The unit-cell parameters were refined from the powder data using the Pawley method and Topas (Topas, Brisbane, Australia) software [34].

3. Results

3.1. Chemical Composition

The chemical composition of dritsite is given in Table 1. The empirical formula was calculated considering crystal-structure data on the basis of (Li + Al + Si) = 6 *apfu*, with the content of interlayer H₂O equal to 2.60 groups pfu. The empirical formula is Li_{1.99}Al_{4.00}Si_{0.01}[(OH)_{12.19}Cl_{1.82}(SO₄)_{0.01}]_{Σ14.02}·2.60H₂O. The ideal formula is Li₂Al₄(OH)₁₂Cl₂·3H₂O, which requires Li₂O 6.63, Al₂O₃ 45.23, H₂O 35.97, Cl 15.72, –O=Cl – 3.55, total 100 wt. %.

Table 1. Chemical data (in wt. %) for dritsite.

Constituent	Mean	Range	Standart Deviation
Li ₂ O	6.6		
Al ₂ O ₃	45.42	45.20–45.67	0.23
SiO ₂	0.11	0.05–0.25	0.08
SO ₃	0.21	0.00–0.47	0.18
Cl	14.33	14.14–14.46	0.13
H ₂ O _{calc.} *	34.86		
–O=Cl	–3.24		
Total	98.29		

Note: * Calculated taking into account the OH content required by electroneutrality and the amount of H₂O groups determined from the crystal-structure study.

3.2. Raman Spectroscopy

The Raman spectra of dritsite are shown in Figure 3 and the assignment of the bands is provided in Table 2. The spectra contain several bands in the range from 3200 to 3600 cm^{–1}, corresponding

to the O–H stretching vibrations. Raman bands observed around 940–980 and 727–745 cm^{-1} are assigned to $\text{Al}\cdots\text{O–H}$ and $\text{Li}\cdots\text{O–H}$ bending vibrations involving OH groups that form stronger (to O atoms) and weaker (to Cl^- anions) hydrogen bonds, respectively. The bands in the ranges 560–599 and 461–464 cm^{-1} are assigned to the $\text{Al}\cdots\text{O}$ and $\text{Li}\cdots\text{O}$, and $\text{Al}\cdots\text{O}$ stretching vibrations, respectively [35–37]. The bands below 400 cm^{-1} correspond to the lattice modes.

Considering the observed low intensity of the band at 1047 cm^{-1} (Figure 3a), it was assigned to the combination mode ($594 + 461 = 1055 \text{ cm}^{-1}$, which differs from the value of 1047 cm^{-1} by the magnitude of the anharmonic shift of 8 cm^{-1}). The assignment of this band to carbonate groups seems unlikely due to the absence of the ν_1 band of the CO_3^{2-} anion in the spectrum (Table 2). It is worth noting that ν_1 bands of the CO_3^{2-} anion are found around 1055–1057 cm^{-1} for stichtite-3R and stichtite-2H, $\text{Mg}_6\text{Cr}_2(\text{OH})_{16}\text{CO}_3(\text{H}_2\text{O})_4$ [38,39], and at 1062 cm^{-1} (stronger) and 1046 (weaker) cm^{-1} for quintinite-2T, $\text{Mg}_4\text{Al}_2(\text{OH})_{12}\text{CO}_3(\text{H}_2\text{O})_3$ [40].

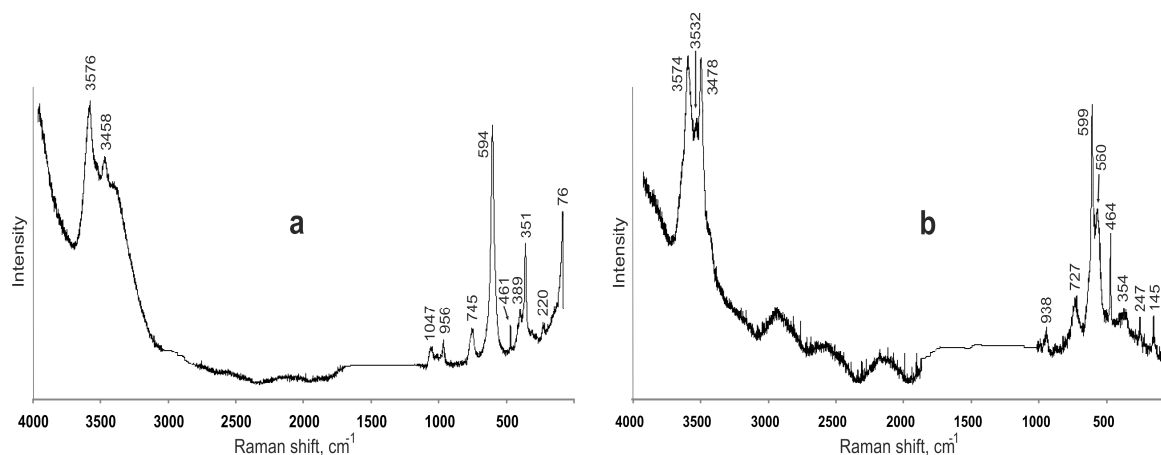


Figure 3. Raman spectra of dritsite recorded from the (a) basal face {001} and (b) lateral face of tabular crystal.

Table 2. Raman bands of the dritsite spectra.

Dritsite		Tentative Assignment
a *	b *	
3576, 3520 sh, 3458	3574, 3532, 3478	O–H stretching of OH groups forming hydrogen bonds with Cl^- (above 3500 cm^{-1}) and O (below 3500 cm^{-1})
3373 sh, 3288 sh	3416	O–H stretching of H_2O groups
1047	-	Combination mode
956	938	$\text{Al}\cdots\text{O–H}$ and $\text{Li}\cdots\text{O–H}$ bending vibrations involving OH groups forming strong hydrogen bonds with O atoms
745	727	$\text{Al}\cdots\text{O–H}$ and/or $\text{Li}\cdots\text{O–H}$ bending vibrations involving OH groups forming weak hydrogen bonds (with Cl^- (?))
594	599, 560	$\text{Al}\cdots\text{O}$ stretching
461	464	$\text{Li}\cdots\text{O}$, $\text{Al}\cdots\text{O}$ stretching
389, 351, 303, 220	354, 247, 145	Lattice modes

* The spectrum recorded from the (a) {001} basal face and (b) the lateral face of a tabular crystal; sh: shoulder; (?): uncertain.

3.3. Single-Crystal X-ray Diffraction and Crystal Structure Determination

The single-crystal X-ray diffraction data were indexed in the $P6_3/mcm$ space group with the unit-cell parameters: $a = 5.0960(3)$, $c = 15.3578(13)$ Å, and $V = 345.4(5)$ Å³ (Table 3). Details on data collection and structure refinement are provided in Table 3. The final structure refinement converged to $R_1 = 0.0885$ for 250 unique observed reflections with $I > 2\sigma(I)$. Site occupancies of the Al, Li, and O atoms of the gibbsite-based layer (Figure 4) were found to be close to 100%, and therefore fixed, while occupancies of the interlayer sites were refined. The position of the H atom in the double hydroxide layer was determined from Fourier electron-density maps and was refined with no imposed restraints on the O–H distances and their geometry. The refined O–H distances of 0.94 Å are consistent with the O–H distances observed in neutron-diffraction studies [41]. Anisotropic displacement parameters were refined only for Al, Li, and O of the gibbsite-based layer and for the rest of the atoms an isotropic approximation was used. Atom coordinates, site occupancies, and displacement parameters are given in Table 4. Selected interatomic distances are provided in Table 5. A crystallographic information file (CIF) for dritsite is available as Supplementary Materials (see below).

Table 3. Crystal data, data collection information, and structure refinement parameters for dritsite.

Crystal Data	
Crystal system	Hexagonal
Space group	$P6_3/mcm$
Unit-cell dimensions a, c (Å)	5.0960(3), 15.3578(13)
Unit-cell volume (Å ³)	345.4(5)
Structural formula, Z	$\text{Li}_2\text{Al}_4(\text{OH})_{12}\text{Cl}_2(\text{H}_2\text{O})_{2.6}$, Z = 1
Absorption coefficient (mm ^{−1})	0.762
Data Collection	
Diffractometer	Xcalibur S CCD
Temperature (K)	293
Radiation, wavelength (Å)	MoK α , 0.71073
θ range for data collection (°)	2.65–32.71
h, k, l ranges	−7→7, −7→7, −22→23
Axis, frame width (°), time per frame (s)	ω , 1, 30
Reflections collected	6039
Unique reflections (R_{int})	257 (0.1035)
Unique reflections $F > 2\sigma(F)$	250
Data completeness to θ_{max} (%)	98.8
Structure Refinement	
Refinement method	Full-matrix least-squares on F^2
Weighting coefficients, a, b	0.199700, 1.606800
Data/restraints/parameters	257/1/43
R_1 [$F > 4\sigma(F)$], wR_2 [$F > 4\sigma(F)$]	0.0885, 0.2606
R_1 all, wR_2 all	0.0910, 0.2648
Goodness-of-fit on F^2	1.053
Largest diff. peak and hole (\AA^{-3})	0.82, −0.67

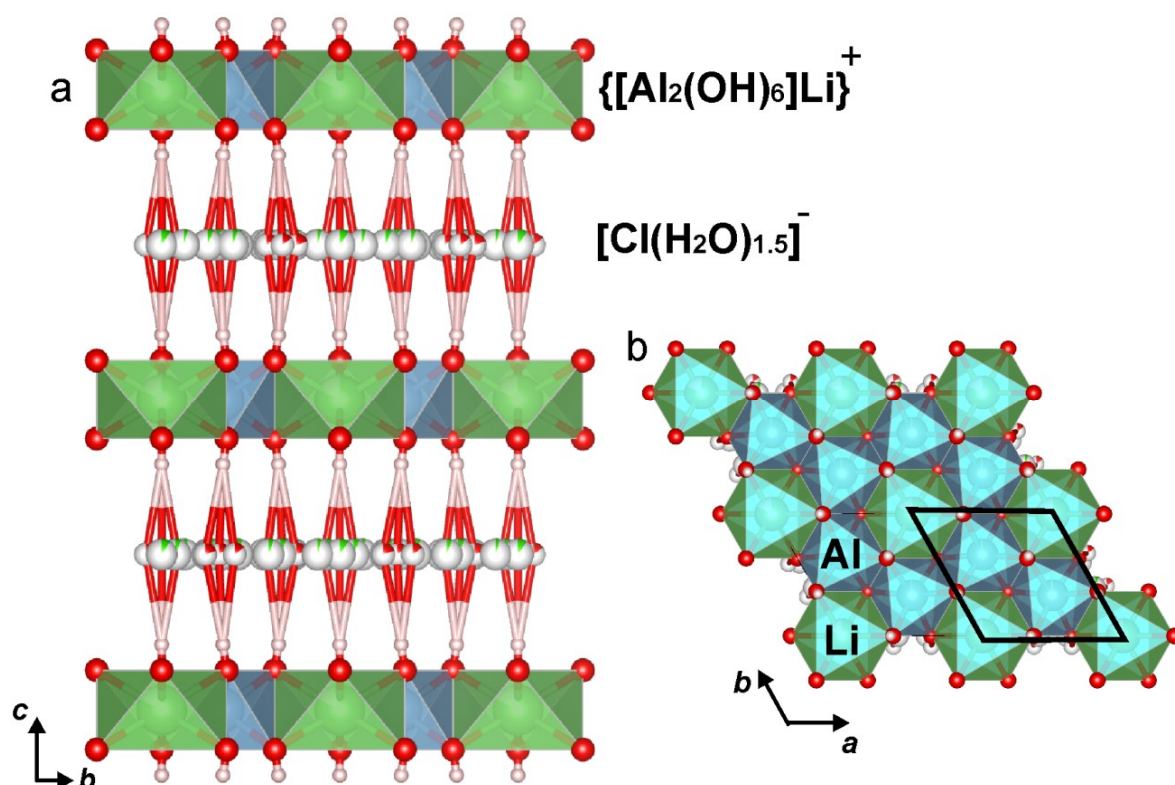


Figure 4. The crystal structure of dritsite-2H (a) and gibbsite-based layer as its part (b); the unit cell is outlined.

Table 4. Atom coordinates, equivalent isotropic displacement parameters (\AA^2), and site occupancies for dritsite-2H.

Atom	W.P.	x	y	z	U_{eq}	s.o.f	s.s. ref (\bar{e})	Assigned Site Populations
Octahedral (gibbsite-based) layer								
Al	4d	1/3	2/3	0	0.0128(3)	1 *	48	Al _{4.0}
Li	2b	0	0	0	0.034(6)	1 *	6	Li _{2.0}
O1	12k	0	0.3653(4)	0.0635(1)	0.0143(9)	1 *	96	(OH) _{12.0}
H1	12k	0	0.368(12)	0.125(2)	0.015(17)	1 *	12	
Interlayer components								
O2	6g	0	0.416(14)	1/4	0.04(2)	0.12(4)	5.8	(H ₂ O) _{2.6}
O3	12j	−0.220(10)	0.687(9)	1/4	0.042(13)	0.16(3)	15.4	
Cl11	6g	0	0.11(3)	1/4	0.04(3)	0.04(3)	4.1	Cl ₂
Cl12	2a	0	0	1/4	0.02(5)	0.04(6)	1.4	
Cl22	4c	−1/3	1/3	1/4	0.02(4)	0.03(3)	2.0	
Cl23	12j	−0.311(9)	0.456(17)	1/4	0.038(14)	0.046(16)	9.4	
Cl31	6g	0	0.68(3)	1/4	0.00(5)	0.01(3)	1.0	
Cl32	6g	0	0.77(3)	1/4	0.05(3)	0.06(3)	6.1	
Cl33	12j	−0.094(13)	0.566(14)	1/4	0.034(12)	0.045(13)	9.2	

Note: * Fixed during refinement in accordance with chemical composition. W.P. = Wyckoff position; x, y, z: coordinates; U_{eq} : isotropic displacement parameter; s.o.f.: site of occupancy; s.s. ref (\bar{e}) = refined site-scattering value.

Table 5. Selected bond lengths (Å) and angles (°) in the crystal structure of dritsite-2H.

Octahedral (Gibbsite-Like) Layer							
Al–O1 × 6		1.8934(19)		Li–O1 × 6		2.101(3)	
Hydrogen Bonding Scheme							
D–H	<i>d</i> (D–H)	<i>d</i> (H···A)	<DHA	<i>d</i> (D···A)	A		
O1–H1	0.94(4)	2.34(9)	144(7)	3.15(5)	Cl11		
O1–H1	0.94(4)	2.92(9)	130(7)	3.60(5)	Cl11		
O1–H1	0.94(4)	2.69(6)	134(6)	3.417(3)	Cl12		
O1–H1	0.94(4)	2.51(4)	140(3)	3.293(3)	Cl22		
O1–H1	0.94(4)	2.66(6)	136(4)	3.41(3)	Cl23		
O1–H1	0.94(4)	2.21(6)	151(4)	3.06(3)	Cl23		
O1–H1	0.94(4)	2.82(6)	133(4)	3.53(3)	Cl23		
O1–H1	0.94(4)	2.51(11)	141(7)	3.30(7)	Cl31		
O1–H1	0.94(4)	2.60(11)	137(7)	3.36(7)	Cl31		
O1–H1	0.94(4)	2.83(12)	134(6)	3.55(8)	Cl32		
O1–H1	0.94(4)	2.53(12)	139(6)	3.29(8)	Cl32		
O1–H1	0.94(4)	2.33(6)	146(6)	3.159(19)	Cl33		
O1–H1	0.94(4)	2.50(6)	140(6)	3.274(19)	Cl33		
O1–H1	0.94(4)	2.99(6)	130(6)	3.660(19)	Cl33		
O1–H1	0.94(4)	1.94(4)	173(8)	2.877(7)	O2		
O1–H1	0.94(4)	2.03(7)	160(6)	2.94(2)	O3		
Cl–H Distances							
Interlayer prism A1		Interlayer prism A2		Interlayer prism A3			
Cl12–H1 × 6	2.69(4)	Cl22–H1 × 6	2.51(3)	Cl31–H1 × 2	2.51(5)	Cl33–H1 × 2	2.33(4)
<Cl12–H1>	2.69	<Cl22–H1>	2.51	Cl31–H1 × 4	2.60(3)	Cl33–H1 × 2	2.50(3)
Cl11–H1 × 4	2.92(5)	Cl21–H1 × 2	2.67(4)	<Cl31–H1>	2.57	Cl33–H1 × 2	2.99(3)
Cl11–H1 × 2	2.34(4)	Cl21–H1 × 2	2.20(3)	Cl32–H1 × 4	2.53(3)	<Cl33–H1>	2.61
<Cl11–H1>	2.73	Cl21–H1 × 2	2.82(3)	Cl32–H1 × 2	2.83(5)		
		<Cl21–H1>	2.56	<Cl32–H1>	2.63		

3.4. Powder X-ray Diffraction

The indexed powder X-ray diffraction data are given in Table 6. The obtained data show a good agreement with the Joint Committee on Powder Diffraction-International Centre for Diffraction Data (JCPDS-ICDD), card #01-087-1768, of the synthetic analogue of dritsite obtained in previous work [4] (Table 6). The unit-cell parameters refined from the powder data are as follows: $P6_3/mcm$ (#193), $a = 5.0992(10)$, $c = 15.3644(14)$ Å, and $V = 345.98(12)$ Å³.

The powder pattern recorded for dritsite contains reflections characteristic of the 2H hexagonal layer stacking sequence. The reflection with $d_{010} = 4.422$ Å (Table 6) is the evidence of cation ordering according to the $\sqrt{3} \times \sqrt{3}$ superstructure in the xy plane, which is typical of LiAl₂-based LDHs [5–8,18,19].

Table 6. Powder X-ray diffraction data for dritsite-2H.

Dritsite-2H (This Study)							Synthetic Analogue of Dritsite-2H* [4]	
I_{meas}	d_{meas} (Å)	I_{calc}	d_{calc} (Å)	h	k	L	I_{meas}	d_{meas} (Å)
100	7.68	100	7.68	0	0	2	100	7.65
61	4.422	15	4.417	0	1	0	11	4.413
99	3.832	34	3.840	0	0	4	60	3.823
		20	3.829	0	1	2		
4	2.899	3	2.898	0	1	4	4	2.890
30	2.561	5	2.560	0	0	6	5	2.549
8	2.516	8	2.515	1	1	1	10	2.513
2	2.421	4	2.420	1	1	2	4	2.417
25	2.283	23	2.283	1	1	3	25	2.279
3	2.216	1	2.215	0	1	6	2	2.207
14	2.124	12	2.124	1	1	4	14	2.120
		>1	2.122	0	2	2		
19	1.963	10	1.962	1	1	5	13	1.958
7	1.920	>1	1.920	0	0	8	2	1.911
	1.914	2	1.914	0	2	4		
20	1.807	14	1.807	1	1	6	16	1.802
7	1.672	2	1.672	0	2	6	2	1.668
2	1.632	1	1.631	2	1	2	1	1.630
1	1.587	1	1.587	2	1	3	<1	1.585
13	1.534	12	1.534	1	1	8	12	1.529
19	1.472	8	1.472	0	3	0	9	1.471
26	1.445	10	1.446	0	3	2	12	1.445

Note: * JCPDS-ICDD, #01-087-1768. The strongest lines are given in bold.

4. Discussion

4.1. Crystal Structure of Dritsite-2H

In general, the crystal structure of dritsite is similar to those of other hydrotalcite supergroup members. It is layered and is composed from alternating positively charged metal-hydroxide layers and negatively charged interlayers (Figure 4a). As the symmetry of dritsite is hexagonal and the unit cell contains two layers, the polytype should be identified as 2H, in accordance with the polytype nomenclature [42]). The specific feature of dritsite is that its alumohydroxide layers are dioctahedral (i.e., gibbsite-based) with octahedral voids occupied by Li atoms (Figure 4b). It is worth noting that the single-crystal structure refinement of dritsite-2H is the first for the family of LiAl_2 -LDHs, because neither synthetic species nor akopovaite were found in crystals suitable for such a study. In the crystal structure of dritsite the octahedral layers contain two symmetrically independent cation sites occupied by Li with $\langle \text{Li-O} \rangle = 2.101$ Å and Al with $\langle \text{Al-O} \rangle = 1.893$ Å (Table 5). The structural formula of the octahedral layer can be written as $[\{\text{Al}_2(\text{OH})_6\}\text{Li}]^+$ [18], which reflects that the layer is gibbsite-like with Li occupying octahedral vacancies.

The arrangement of Cl^- anions and H_2O groups in the interlayer space of dritsite shows statistical disorder (Figure 5). The general architecture of the interlayer arrangement of dritsite is principally different from that of carbonate hydrotalcite supergroup minerals, namely quintinite, hydrotalcite, pyroaurite, stichtite, takovite, and zaccagnaite [38,43–50], as shown in Figure 5c,d. In accordance with the approach by Bookin and Drits [23], the interlayer space can be considered as consisting of trigonal prisms formed by H atoms occupying the H1 site of the metal-hydroxide layers (Figure 5e,f). The interlayer consists of three types of such prisms, namely A1, A2, and A3, hosting Cl atoms at their centers and H_2O groups in the vertical edge middle points (Figure 5e). The Cl–H1 distances range from 2.51 to 2.99 Å, while the H_2O –H1 distances are much shorter (1.94–2.03 Å) (Table 5). Similar

results with Cl^- sitting in a trigonal prismatic environment of $6(\text{OH})^-$ groups have been obtained for $\text{LiAl}_2\text{-Cl}$ LDHs using ^{35}Cl nuclear magnetic resonance (NMR) spectroscopy and molecular dynamic modelling, although a distorted octahedral environment caused by $4(\text{OH})^-$ and $2(\text{H}_2\text{O})^0$ has also been suggested by other authors [51], however was not observed in our study.

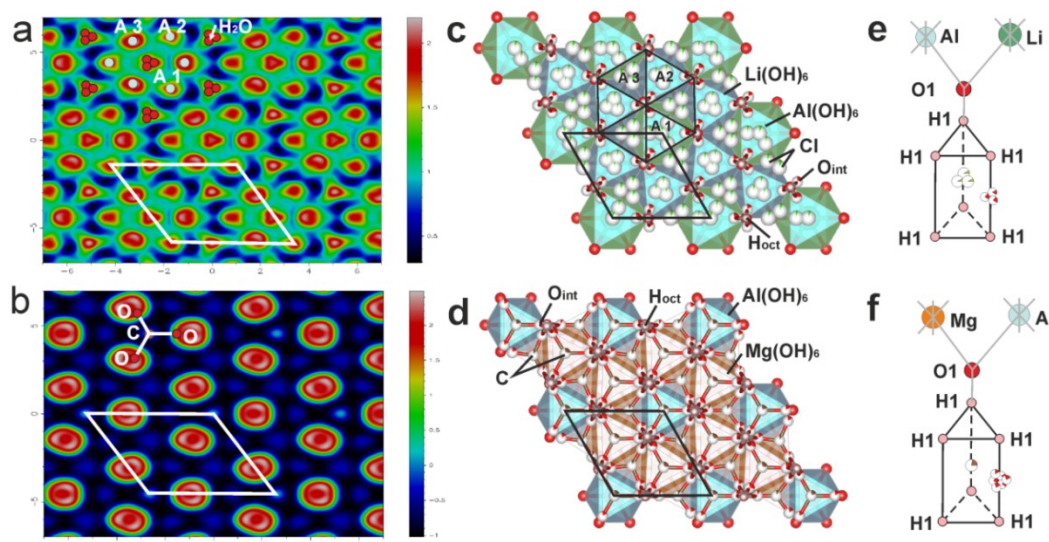


Figure 5. Electron density maps at the interlayer level for dritsite-2H (a) and quintinite-2T, $[\text{Mg}_4\text{Al}_2(\text{OH})_{12}][(\text{CO}_3)(\text{H}_2\text{O})_3]$ (b); the architecture of the interlayer space superimposed upon metal-hydroxide layers for dritsite-2H (c) and quintinite-2T (d); the arrangement of interlayer species in trigonal prisms built by H atoms of the upper and lower metal-hydroxide layers for dritsite-2H (e) and quintinite-2T (f).

4.2. Comparison to Other Hydrotalcite Supergroup Minerals and Synthetic Compounds

Hydrotalcite supergroup members have been described in various geological settings, but it is important for the present study that naturally occurring LDHs, namely quintinite and two unnamed natural phases (the sulphate and sulphate-carbonate analogues of quintinite), were reported from the saline deposits in the central part of the pre-Caspian depression (West Kazakhstan) by Drits et al. [22]. Recently, another hydrotalcite supergroup mineral—motukoreaite, $[\text{Mg}_6\text{Al}_3(\text{OH})_{18}][\text{Na}(\text{H}_2\text{O})_6][\text{SO}_4]_2 \cdot n\text{H}_2\text{O}$; $n \ll 6$ —was reported from the Kłodawa Salt Dome (Central Poland), where it forms during diagenetic and metamorphic processes [52]. Our finding of dritsite shows that hydrotalcite supergroup minerals may be much more abundant in saline deposits than previously thought.

This study, the results of which are reported herein, is the first single-crystal structure refinement of $\text{LiAl}_2\text{-LDH}$, though synthetic $\text{LiAl}_2\text{-LDHs}$ are well-known and have been structurally characterized using powder X-ray diffraction or neutron diffraction on fine-grained materials accompanied by Rietveld structure refinements. It has been shown that synthetic $\text{LiAl}_2\text{-LDHs}$ form two polytypic modifications: 1M, space group $\text{C2}/m$, $a \sim 5.10$, $b \sim 8.88$, $c \sim 7.80$ Å, $\beta \sim 103^\circ$, and 2H, space group $\text{P6}_3/\text{mcm}$ (or $\text{P6}_3/m$), $a \sim 5.10$, and $c \sim 15.36$ Å [5–8]. Both modifications are characterized by the strong Li–Al ordering, with Li occupying vacancies in the gibbsite-like layered structure and different layer-stacking sequences. As noted above, natural dritsite is found as a 2H polytype. Among natural LDHs, i.e., hydrotalcite supergroup minerals, the $\text{LiAl}_2\text{-members}$ show structural similarities with the quintinite group members ($\text{M}^{2+}_2\text{M}^{3+}\text{-LDH}$) due to the same scheme of cation ordering, i.e., the formation of the $\sqrt{3} \times \sqrt{3}$ superstructure (Figure 5). In particular, dritsite-2H is isotypic to chlormagaluminate-2H, considering the following substitution scheme: $[\text{Mg}_2\text{Al}(\text{OH})_6]^+$ (brucite-type layers) $\rightarrow [\text{Al}_2\text{Li}(\text{OH})_6]^+$ (gibbsite-based layers with Li^+ cations filling octahedral voids) (Table 7). Despite the structural isotypism of $\text{LiAl}_2\text{-based}$ and quintinite group members, they demonstrate essential crystal chemical

differences. The hydrotalcite supergroup members with di- and trivalent cations have fully occupied M sites (M^{2+} , M^{3+} or $M^{2+,3+}$) within brucite-type layers and the layer charge controlled by the number of trivalent cations. For the LiAl_2 -based members, Li occupies vacancies in the gibbsite-type structure and the charge of the layer is controlled by the Li content. For instance, a hypothetical member with $\text{Li}:\text{Al} = 1:4$, i.e., with $[\text{Li}_{0.5}\text{Al}_2(\text{OH})_6]^{0.5+}$ layers with half-occupied Li sites, is quite possible, whereas natural di- and trivalent member samples with the ratio $M^{2+}:M^{3+} = 4:1$ have not yet been found. In principle, the formation of new Li-deficient members is possible due to Li^+ leaching from gibbsite-based layers [18], which is a specific feature of synthetic LiAl_2 -LDHs. The strong crystal-chemical difference of natural LiAl_2 -LDHs from LDHs with di- and trivalent cations suggests their separation into a separate group within the hydrotalcite supergroup.

Table 7. Comparative data of dritsite, its synthetic analogue, and structurally studied, related hydrotalcite supergroup minerals chlormagaluminite and quintinite.

Phase	Cl-LDHs			CO ₃ -LDHs	
	Dritsite	Synthetic analogue of dritsite	Chlormagaluminite	Quintinite *	
Symbol		$\text{LiAl}_2\text{-Cl}$	$\text{Mg}_2\text{Al-Cl}$	$\text{Mg}_2\text{Al-CO}_3$	
Polytype	2H	2H	2H	2T	2H
Crystal chemical formula	$[\text{Al}_4\text{Li}_2(\text{OH})_{12}][\text{Cl}_2(\text{H}_2\text{O})_3]$		$[\text{Mg}_4\text{Al}_2(\text{OH})_{12}][\text{Cl}_2(\text{H}_2\text{O})_3]$	$[\text{Mg}_4\text{Al}_2(\text{OH})_{12}][(\text{CO}_3)(\text{H}_2\text{O})_3]$	
Crystal system	Hexagonal			Trigonal	Hexagonal
Space group	$P6_3/mcm^{**}$			$P-3c1$	$P6_3/mmc$
a , Å	5.0960(3)	5.0963(3)	5.268(3)	5.2720(6)	3.0455(10)
c , Å	15.3578(13)	15.2919(9)	15.297(8)	15.113(3)	15.125(7)
β , °	90	90	90	90	90
V , Å ³	345.4(5)	344.0	367.6(4)	363.8	121.5
The strongest lines in the PXRD pattern: d , Å (I , %)	7.68 (100)	7.65 (100)	7.72 (100)	7.56 (100)	7.57 (100)
	4.422 (61)	3.823 (60)	3.856 (38)	3.778 (58)	3.785 (57)
	3.832 (99)	2.279 (25)	2.350 (38)	2.600 (14)	2.600 (11)
	2.561 (30)	2.210 (14)	2.179 (34)	2.519 (10)	2.524 (10)
	2.283 (25)	1.958 (13)	1.843 (29)	2.489 (9)	2.492 (8)
	1.445 (26)	1.802 (16)	1.558 (16)	1.987 (7)	1.824 (6)
Reference	This study	[4]	[53]	[47]	[47]

Note: * Powder X-ray diffraction patterns were calculated using crystal structure data. ** The crystal structure of synthetic analogue of dritsite has been solved in $P6_3/m$ and $P6_3/mcm$ space groups, with better agreement in the latter [4].

It is important to note that synthetic LiAl_2 -LDHs have always been considered under the term “layered double hydroxides” [4–19], because in terms of both their chemistry and crystal structure they satisfy the criteria of LDHs. Therefore, we suggest that dritsite should be included into the hydrotalcite supergroup [3] as the first representative of a new group. At the same time, LiAl_2 -LDHs, $[\text{LiAl}_2(\text{OH})_{12}]^{2+}[\text{A}_x^{2-/x}(\text{H}_2\text{O})_n]$ (where A—anion; x —anion *apfu*, 2/ x —anion charge), are structurally closely related to the chalcoalumite group minerals, $[\text{M}^{2+}\text{Al}_4(\text{OH})_{12}][(\text{TO}_3/\text{SO}_4)_m(\text{H}_2\text{O})_n]$, where species-defining $M = \text{Ni}$, Zn or Cu^{2+} ; $T = \text{N}^{3+}$ or V^{5+} ; $m = 1, 2$; $2 < n < 12$ (Table 8). The crystal structures of both types of compounds consist of gibbsite-based dioctahedral layers, with Li^+ filling all octahedral voids or M^{2+} filling one half of octahedral voids. The chalcoalumite group minerals have not been considered as a part of the hydrotalcite supergroup, mainly due to the vacancies in the octahedral layers [3]. However, the addition of LiAl_2 -LDHs to the hydrotalcite supergroup could change the approach to vacancies in the octahedral layer from the viewpoint of mineral nomenclature.

This is because the hypothetical occupancy of the Li site of 80% in dritsite does not lead to the formation of a new mineral species, but results in the formation of 20% vacancies in the metal-hydroxide layers. The structural similarity between dritsite and chalcoalumite group minerals indicates that the place of the chalcoalumite group members in mineral nomenclature may be reconsidered with their insertion into the hydrotalcite supergroup, i.e., recognized as LDHs [54]).

Table 8. The chemical formula and crystallographic parameters of the chalcoalumite group minerals, $[M^{2+}Al_4(OH)_{12}][(TO_3/SO_4)_m(H_2O)_n]$, where M^{2+} - species-defining cation; $T = N^{3+}$ or V^{5+} ; $m = 1, 2$; $2 < n < 12$ [55].

Title	M^{2+}	A	n	Space Group	a, Å	b, Å	c, Å	β , °	Reference
“Nickelalumite”	Ni	SO ₄	3	$P2_1/n$	10.2567	8.8815	17.0989	95.548	[56,57]
Kyrgyzstanite	Zn	SO ₄	3	$P2_1/n$	10.246	8.873	17.220	96.41	[58]
Chalcoalumite	Cu	SO ₄	3	$P2_1/n$	10.228	8.929	17.098	95.800	[55,59,60]
Alvanite	Zn	VO ₃	2	$P2_1/n$	17.808	5.132	8.881	92.11	[61]
Ankinovichite	Ni	VO ₃	2	$P2_1/n$	17.8098	5.1228	8.8665	92.141	[62]
Mbobomkulite	Ni	NO ₃	3	unknown	10.171	8.865	17.145	95.37	[63]
Hydro-Mbobomkulite	Ni	NO ₃	12	unknown	10.145	17.155	20.870	90.55	[63]

5. Conclusions

Herein we reported on the new mineral species dritsite, the representative of natural Li_2Al -LDHs. Its discovery essentially extends the current knowledge on natural LDHs, which until now included only di- and trivalent cations. It is also important that we report on the first single-crystal refinement performed on Li_2Al -LDHs, since all previous studies were focused on synthetic fine-grained powdered material. The crystal–chemical uniqueness of Li_2Al -LDH minerals suggests that they should be placed into a separate group within the hydrotalcite supergroup.

The study also points to the need for detailed and careful crystal–chemical comparison of the chalcoalumite group of minerals with members of hydrotalcite supergroup, considering the new crystal chemistry introduced by the approval of a new $LiAl_2$ -LDH mineral-dritsite.

Supplementary Materials: The crystallographic information file (cif) is available online at <http://www.mdpi.com/2075-163X/9/8/492/s1>.

Author Contributions: Conceptualization, E.S.Z., I.V.P., I.I.C.; methodology, E.S.Z., I.V.P.; investigation, E.S.Z., I.V.P., I.I.C., E.P.C., V.O.Y., Y.V.B., D.I.B., N.V.C., N.V.Z., V.N.B.; writing—original draft preparation, E.S.Z., I.V.P., N.V.C., V.N.B.; writing—review and editing, E.S.Z., I.V.P., N.V.C., N.V.Z., S.V.K.; visualization, E.S.Z.

Funding: This research was funded by grants of the President of the Russian Federation for leading scientific schools, NSh-3079.2018.5 for E.S.Z. and S.V.K. (structural study), and Russian Fund for Basic Research, 18-05-00046 for I.I.C., E.P.C. (field work).

Acknowledgments: The research has been carried out using facilities of XRD and Geomodel Research Centers of Saint Petersburg State University. We would like to thank three anonymous reviewers and Stuart Mills for valuable comments that improved the quality of the manuscript.

Conflicts of Interest: The authors declare no conflict of interest.

References

1. Rives, V. *Layered Double Hydroxides: Present and Future*; Nova Science Publishers: New York, NY, USA, 2001.
2. Evans, D.G.; Slade, R.C.T. Structural aspects of layered double hydroxides. In *Layered Double Hydroxides*; Duan, X., Evans, D.G., Eds.; Springer: Berlin, Germany, 2006; Volume 119, pp. 1–87.
3. Mills, S.J.; Christy, A.G.; Génin, J.-M.R.; Kameda, T.; Colombo, F. Nomenclature of the hydrotalcite supergroup: natural layered double hydroxides. *Miner. Mag.* **2012**, *76*, 1289–1336. [CrossRef]

4. Besserguenev, A.V.; Fogg, A.M.; Francis, R.J.; Price, S.J.; O'Hare, D.; Isupov, V.P.; Tolochko, B.P. Synthesis and structure of the gibbsite intercalation compounds $[\text{LiAl}_2(\text{OH})_6]\text{X}$ $\{\text{X} = \text{Cl}, \text{Br}, \text{NO}_3\}$ and $[\text{LiAl}_2(\text{OH})_6]\text{Cl}\cdot\text{H}_2\text{O}$ using synchrotron X-ray and neutron powder diffraction. *Chem. Mater.* **1997**, *9*, 241–247. [[CrossRef](#)]
5. Britto, S.; Kamath, P.V. Structure of Bayerite-Based Lithium–Aluminum Layered Double Hydroxides (LDHs): Observation of Monoclinic Symmetry. *Inorg. Chem.* **2009**, *48*, 11646–11654. [[CrossRef](#)] [[PubMed](#)]
6. Britto, S.; Kamath, P.V. Polytypism in the lithium–aluminum layered double hydroxides: the $[\text{LiAl}_2(\text{OH})_6]^+$ layer as a structural synthon. *Inorg. Chem.* **2011**, *50*, 5619–5627. [[CrossRef](#)] [[PubMed](#)]
7. Britto, S.; Thomas, G.S.; Kamath, P.V.; Kannan, S. Polymorphism and structural disorder in the carbonate containing layered double hydroxide of Li with Al. *J. Phys. Chem.* **2008**, *112*, 9510–9515. [[CrossRef](#)]
8. Nagendran, S.; Kamath, P.V. Structure of the chloride- and bromide-intercalated Layered Double Hydroxides of Li and Al—interplay of coulombic and hydrogen-bonding interactions in the interlayer gallery. *Eur. J. Inorg. Chem.* **2013**, *26*, 4686–4693. [[CrossRef](#)]
9. Niksch, A.; Pöllmann, H. Synthesis and characterization of a $[\text{Li}_{0+x}\text{Mg}_{2-2x}\text{Al}_{1+x}(\text{OH})_6][\text{Cl}\cdot m\text{H}_2\text{O}]$ Solid solution with $x = 0$ –1 at different temperatures. *Nat. Resour. J.* **2017**, *8*, 445–459.
10. Devyatkina, E.T.; Kotsupalo, N.P.; Tomilov, N.P.; Berger, A.S. On the lithium carbonate-hydroxyl-aluminate. *Zhurnal Neorg. Khimii.* **1983**, *28*, 1420–1425. (In Russian)
11. Drewien, C.A.; Eatough, M.O.; Tallant, D.R.; Hills, C.R.; Buchheit, R.G. Lithium-aluminum-carbonate-hydroxide hydrate coatings on aluminum alloys: composition, structure, and processing bath chemistry. *J. Mater. Res.* **1996**, *11*, 1507–1513. [[CrossRef](#)]
12. Hou, X.; Kirkpatrick, R.J. Thermal Evolution of the Cl^- - LiAl_2 Layered Double Hydroxide: A Multinuclear MAS NMR and XRD Perspective. *Inorg. Chem.* **2001**, *40*, 6397–6404. [[CrossRef](#)]
13. Huang, L.; Wang, J.; Gao, Y.; Qiao, Y.; Zheng, Q.; Guo, Z.; Zhao, Y.; O'Hare, D.; Wang, Q. Synthesis of LiAl_2 -layered double hydroxides for CO_2 capture over a wide temperature range. *J. Mater. Chem.* **2014**, *2*, 18454–18462. [[CrossRef](#)]
14. Isupov, V.P. Intercalation compounds of aluminium hydroxide. *J. Struct. Chem.* **1999**, *40*, 672–685. [[CrossRef](#)]
15. Isupov, V.P.; Chupakina, L.E.; Tarasov, K.A.; Shestakova, N.Yu. Synthesis of superfine carbonate form of Li–Al double hydroxide from sodium hydroaluminocarbonate. *Chem. Sustain. Dev.* **2007**, *15*, 63–69.
16. Serna, C.J.; White, J.L.; Hem, S.L. Hydrolysis of aluminium-tri-(sec-butoxide) in ionic and nonionic media. *Clay Clay Miner.* **1977**, *25*, 384–391. [[CrossRef](#)]
17. Serna, C.J.; Rendon, J.L.; Iglesias, J.E. Crystal-chemical study of layered $[\text{Al}_2\text{Li}(\text{OH})_6]^+\cdot n\text{H}_2\text{O}$. *Clay Clay Miner.* **1982**, *30*, 180–184. [[CrossRef](#)]
18. Sissoko, I.; Iyagba, E.T.; Sahai, I.; Biloen, P. Anion intercalation and exchange in $\text{Al}(\text{OH})_3$ -derived compounds. *J. Solid State Chem.* **1985**, *60*, 283–288. [[CrossRef](#)]
19. Thiel, J.P.; Chiang, C.K.; Poeppelmeier, K.R. Structure of $\text{LiAl}_2(\text{OH})_7\cdot\text{H}_2\text{O}$. *Chem. Mater.* **1993**, *5*, 297–304. [[CrossRef](#)]
20. Génin, J.-M.R.; Mills, S.J.; Christy, A.G.; Guérin, O.; Herbillon, A.J.; Kuzmann, E.; Ona-Nguema, G.; Ruby, C.; Upadhyay, C. Mössbauerite, $\text{Fe}^{3+}_6\text{O}_4(\text{OH})_8[\text{CO}_3]\cdot 3\text{H}_2\text{O}$, the fully oxidized 'green rust' mineral from Mont Saint-Michel Bay, France. *Miner. Mag.* **2014**, *78*, 447–465. [[CrossRef](#)]
21. Karpenko, V.Yu.; Pautov, L.A.; Zhitova, E.S.; Agakhanov, A.A.; Krzhizhanovskaya, M.G.; Siidra, O.I.; Rassulov, V.A. Akopovaite, IMA 2018-095. CNMNC Newsletter No. 46, December 2018, page 1186. *Eur. J. Miner.* **2018**, *30*, 1181–1189.
22. Drits, V.A.; Sokolova, T.N.; Sokolova, G.V.; Cherkashin, V.I. New members of hydrotalcite-manasseite group. *Clay Clay Min.* **1987**, *35*, 401–417. [[CrossRef](#)]
23. Bookin, A.S.; Drits, V.A. Polytype diversity of the hydrotalcite-like minerals. I. Possible polytypes and their diffraction patterns. *Clay Clay Min.* **1993**, *41*, 551–557. [[CrossRef](#)]
24. Saalfeld, H.; Wedde, M. Refinement of the crystal structure of gibbsite, $\text{Al}(\text{OH})_3$. *Z. für Krist.* **1974**, *139*, 129–135. [[CrossRef](#)]
25. Zigan, F.; Rothbauer, R. Neutronenbeugungsmessungen am Brucit. *Neues JB Miner. Mon* **1967**, *1967*, 137–143.
26. Kudryashov, A.I. *Verkhnekamskoe Salt Depos.*, 2nd ed.; Epsilon Plus: Moscow, Russia, 2013; pp. 1–368. (In Russian)
27. Chaikovskiy, I.I.; Chaikovskaya, E.V.; Korotchenkova, O.V.; Chirkova, E.P.; Utkina, T.A. Autogenic titanium and zirconium minerals at the Verkhnekamskoe salt deposit. *Geochem. Int.* **2019**, *57*, 184–196. [[CrossRef](#)]
28. Ivanov, A.A.; Voronova, M.L. *Verkhnekamskoe Potash Salt Depos.*; Nedra: Leningrad, Russian, 1975; pp. 1–219.

29. Pekov, I.V.; Zubkova, N.V.; Chaikovskiy, I.I.; Chirkova, E.P.; Belakovskiy, D.I.; Yapaskurt, V.O.; Bychkova, Y.V.; Lykova, I.S.; Britvin, S.N.; Pushcharovsky, D.Y. Krasnoshteinite, IMA 2018-077. CNMNC Newsletter No. 46, December 2018, page 1182. *Eur. J. Miner.* **2018**, *30*, 1181–1189.
30. Mandarino, J.A. The Gladstone–Dale compatibility of minerals and its use in selecting mineral species for further study. *Can. Miner.* **2007**, *45*, 1307–1324. [[CrossRef](#)]
31. *CrysAlis^{Pro}*, version 1.171.37.35; Data Collection and Processing Software for Agilent X-ray Diffractometers; Agilent Technologies UK Ltd.: Oxford, UK, 2014.
32. Sheldrick, G.M. Crystal structure refinement with SHELXL. *Acta Cryst.* **2015**, *C71*, 3–8.
33. Britvin, S.N.; Dolivo-Dobrovolsky, D.V.; Krzhizhanovskaya, M.G. Software for processing of X-ray powder diffraction data obtained from the curved image plate detector of Rigaku RAXIS Rapid II diffractometer. *Zap. Ross. Miner. Obs.* **2017**, *146*, 104–107. (In Russian with English abs.)
34. *Topas*, version 4.2; General Profile and Structure Analysis Software for Powder Diffraction Data. Bruker-AXS: Karlsruhe, Germany, 2009.
35. Brabers, V.A.M. Infrared spectra and ionic ordering of the lithium ferrite–aluminate and chromite systems. *Spectrochim. Acta. A* **1976**, *32*, 1709–1711. [[CrossRef](#)]
36. Khosravi, I.; Yazdanbakhsh, M.; Eftekhari, M.; Haddadi, Z. Fabrication of nano delafossite $\text{LiCo}_{0.5}\text{Fe}_{0.5}\text{O}_2$ as the new adsorbent in efficient removal of reactive blue from aqueous solutions. *Mater. Res. Bull.* **2013**, *48*, 2213–2219. [[CrossRef](#)]
37. Ruan, H.D.; Frost, R.L.; Klopogge, J.T. Comparison of Raman spectra in characterizing gibbsite, bayerite, diasporite and boehmite. *J. Raman Spectrosc.* **2001**, *32*, 745–750. [[CrossRef](#)]
38. Mills, S.J.; Whitfield, P.S.; Wilson, S.A.; Woodhouse, J.N.; Dipple, G.M.; Raudsepp, M.; Francis, C.A. The crystal structure of stichtite, re-examination of barbertonite, and the nature of polytypism in MgCr hydrotalcites. *Am. Miner.* **2011**, *96*, 179–187. [[CrossRef](#)]
39. Zhitova, E.S.; Pekov, I.V.; Chukanov, N.V.; Yapaskurt, V.O.; Bocharov, V.N. Minerals of the stichtite-pyroaurite-iowaite-woodallite system from serpentinites of Terektinsky range, Altay Mountains, Russia. *Russ. Geol. Geoph.* **2019**, in press.
40. Theiss, F.; López, A.; Frost, R.L.; Scholz, R. Spectroscopic characterisation of the LDH mineral quintinite $\text{Mg}_4\text{Al}_2(\text{OH})_{12}\text{CO}_3 \times 3\text{H}_2\text{O}$. *Spectrochim. Acta A* **2015**, *150*, 758–764. [[CrossRef](#)]
41. Jeffrey, G.A. *An Introduction to Hydrogen Bonding*; Oxford University Press: New York, NY, USA, 1997.
42. Guinier, A.; Bokij, G.B.; Boll-Dornberger, K.; Cowley, J.M.; Durovic, S.; Jagodzinski, H.; Krishna, P.; DeWolff, P.M.; Zvyagin, B.B.; Cox, D.E.; et al. Nomenclature of polytype structures. Report of the International Union of Crystallography ad-hoc committee on the Nomenclature of disordered, modulated and polytype structures. *Acta Cryst.* **1984**, *A40*, 399–404. [[CrossRef](#)]
43. Krivovichev, S.V.; Yakovenchuk, V.N.; Zhitova, E.S.; Zolotarev, A.A.; Pakhomovsky, Y.A.; Ivanyuk, G.Y. Crystal chemistry of natural layered double hydroxides. 1. Quintinite-2H-3c from the Kovdor alkaline massif, Kola peninsula, Russia. *Miner. Mag.* **2010**, *74*, 821–832.
44. Krivovichev, S.V.; Yakovenchuk, V.N.; Zhitova, E.S.; Zolotarev, A.A.; Pakhomovsky, Y.A.; Ivanyuk, G.Y. Crystal chemistry of natural layered double hydroxides. 2. Quintinite-1M: First evidence of a monoclinic polytype in M^{2+} – M^{3+} layered double hydroxides. *Miner. Mag.* **2010**, *74*, 833–840.
45. Zhitova, E.S.; Yakovenchuk, V.N.; Krivovichev, S.V.; Zolotarev, A.A.; Pakhomovsky, Y.A.; Ivanyuk, G.Y. Crystal chemistry of natural layered double hydroxides. 3. The crystal structure of Mg, Al-disordered quintinite-2H. *Miner. Mag.* **2010**, *74*, 841–848.
46. Zhitova, E.S.; Ivanyuk, G.Y.; Krivovichev, S.V.; Yakovenchuk, V.N.; Pakhomovsky, Y.A.; Mikhailova, Y.A. Crystal Chemistry of Pyroaurite from the Kovdor Pluton, Kola Peninsula, Russia, and the Långban Fe–Mn deposit, Värmland, Sweden. *Geol. Ore Depos.* **2017**, *59*, 652–661. [[CrossRef](#)]
47. Zhitova, E.S.; Krivovichev, S.V.; Yakovenchuk, V.N.; Ivanyuk, G.Y.; Pakhomovsky, Y.A.; Mikhailova, J.A. Crystal chemistry of natural layered double hydroxides. 4. Crystal structures and evolution of structural complexity of quintinite polytypes from the Kovdor alkaline massif, Kola peninsula, Russia. *Miner. Mag.* **2018**, *82*, 329–346.
48. Zhitova, E.S.; Krivovichev, S.V.; Pekov, I.V.; Greenwell, H.C. Crystal chemistry of natural layered double hydroxides. 5. Single-crystal structure refinement of hydrotalcite, $[\text{Mg}_6\text{Al}_2(\text{OH})_{16}](\text{CO}_3)(\text{H}_2\text{O})_4$. *Miner. Mag.* **2019**, *83*, 269–280.

49. Mills, S.J.; Whitfield, P.S.; Kampf, A.R.; Wilson, S.A.; Dipple, G.M.; Raudsepp, M.; Favreau, G. Contribution to the crystallography of hydrotalcites: The crystal structures of woodallite and takovite. *J. Geosci.* **2012**, *58*, 273–279. [\[CrossRef\]](#)
50. Lozano, R.P.; Rossi, C.; La Iglesia, A.; Matesanz, E. Zaccagnaite-3R, a new Zn–Al hydrotalcite polytype from El Soplaio cave (Cantabria, Spain). *Am. Miner.* **2012**, *97*, 513–523. [\[CrossRef\]](#)
51. Hou, X.; Kalinichev, A.G.; Kirkpatrick, R.J. Interlayer structure and dynamics of Cl–LiAl₂-Layered Double Hydroxides: ³⁵Cl NMR observation and molecular dynamic simulation. *Chem. Mater.* **2002**, *14*, 2078–2085. [\[CrossRef\]](#)
52. Wachowiak, J.; Pieczk, A. Motukoreaite from the Kłodawa Salt Dome, Central Poland. *Miner. Mag.* **2016**, *80*, 277–289. [\[CrossRef\]](#)
53. Zhitova, E.S.; Krivovichev, S.V.; Pekov, I.V.; Yapaskurt, V.O. Crystal Chemistry of Chlormagaluminate, Mg₄Al₂(OH)₁₂Cl₂(H₂O)₂, a Natural Layered Double Hydroxide. *Minerals* **2019**, *9*, 221. [\[CrossRef\]](#)
54. Jensen, N.D.; Duong, N.T.; Bolanz, R.; Nishiyama, Y.; Rasmussen, C.A.; Gottlicher, J.; Steininger, R.; Prevot, V.; Nielsen, U.G. Synthesis and structural characterization of a pure ZnAl₄(OH)₁₂(SO₄)·2.6H₂O Layered Double Hydroxide. *Inorg. Chem* **2019**, in press. [\[CrossRef\]](#)
55. Hawthorne, F.C.; Cooper, M.A. The crystal structure of chalcoalumite: mechanisms of Jahn-Teller-driven distortion in [6]Cu²⁺-containing oxysalts. *Miner. Mag.* **2013**, *77*, 2901–2912. [\[CrossRef\]](#)
56. Uvarova, Yu. A.; Sokolova, E.; Hawthorne, F.C.; Karpenko, V.V.; Agakhanov, A.A.; Pautov, L.A. The crystal chemistry of the “nickelalumite”-group minerals. *Can. Miner.* **2005**, *43*, 1511–1519. [\[CrossRef\]](#)
57. Karpenko, V.V.; Agakhanov, A.A.; Pautov, L.A.; Dikaya, T.V.; Bekenova, G.K. New occurrence of nickelalumite on Kara-Chagyr, South Kirgizia. *New Data Miner.* **2004**, *39*, 32–39.
58. Agakhanov, A.A.; Karpenko, V.Y.; Pautov, L.A.; Uvarova, Y.A.; Sokolova, E.; Hawthorne, F.C.; Bekenova, G.K. Kyrgyzstanite, ZnAl₄(SO₄)(OH)₁₂(H₂O)₃—A new mineral from the Kara-Tangi, Kyrgyzstan. *New Data Miner.* **2005**, *40*, 23–28.
59. Williams, S.; Khin, B.S. Chalcoalumite from Bisbee, Arizona. *Miner. Rec.* **1971**, *2*, 126–127.
60. Larsen, E.S.; Vassar, H.E. Chalcoalumite, a new mineral from Bisbee, Arizona. *Am. Miner.* **1925**, *10*, 79–83.
61. Pertlik, F.; Dunn, P.J. Crystal structure of alvanite, (Zn,Ni)Al₄(VO₃)₂(OH)₁₂·2H₂O, the first example of an unbranched zweier-single chain vanadate in nature. *Neues JB Miner. Mon.* **1990**, *9*, 385–392.
62. Karpenko, V.V.; Pautov, L.A.; Sokolova, E.; Hawthorne, F.C.; Agakhanov, A.A.; Dikaya, T.V.; Bekenova, G.K. Ankinovichite, nickel analogue of alvanite, a new mineral from Kurunsak (Kazakhstan) and Kara-Chagyr (Kirgizia). *Zap. RMO* **2004**, *133*, 59–70.
63. Martini, J.E.J. Mbobomkulite, hydrombobomkulite, and nickelalumite, new minerals from Mbobo Mkulu cave, eastern Transvaal. *Ann. Geol. Surv. S. Afr.* **1980**, *14*, 1–10.

